Calibration of a Fully Polarimetric Microwave Radiometer Using a Digital Polarimeric Noise Source

Boon H Lim and Christopher S Ruf
University of Michigan
Ann Arbor, MI USA
734-764-6561 (V), 734-936-0503 (F),
bhlim@umich.edu / cruf@umich.edu (E)

Abstract – The Correlated Noise Calibration Standard (CNCS) is an electronic device that generates two channels of broadband microwave noise with a programmable degree of complex correlation. It can supply signals to the input of a microwave radiometer with independently variable vertical, horizontal, 3rd and 4th Stokes brightness temperatures. An X-Band version of the CNCS has been evaluated with the NASA Goddard Airborne Earth Science Microwave Imaging Radiometer (AESMIR). AESMIR measurements were made with a highly over constrained set of CNCS polarimetric states. This allows for the simultaneous solution of both non-ideal characteristics of the CNCS system as well as of the complete polarization mixing calibration equation for AESMIR. Absolute calibration accuracy of AESMIR is estimated to be 0.2 K for its 3rd and 4th Stokes channels.

Keywords- Microwave Radiometry, Calibration, Polarimetric Radiometry, Noise Generators

I. INTRODUCTION

A new type of calibration standard has been developed which produces a pair of microwave noise signals to aid in the characterization and calibration of correlating radiometers. The Correlated Noise Calibration Standard (CNCS) is able to generate pairs of broad bandwidth stochastic noise signals with a wide variety of statistical properties [1]. It can be used with synthetic aperture interferometers to generate specific visibility functions. It can be used with fully polarimetric radiometers to generate specific 3rd and 4th Stokes brightness temperatures. It can be used with spectrometers to generate specific power spectra and autocorrelations. The CNCS can also generate any of these naturally occurring radiometric signals superimposed on realistic radio frequency interference (RFI) signal, to test the susceptibility/tolerance of a radiometer to RFI.

A prototype CNCS has been built at 10.7 GHz [1]. A block diagram is presented in Fig. 1. Briefly, the CNCS utilizes a commercial dual channel arbitrary waveform generator (AWG) that is capable of producing signals up to 125 MHz. Noise generation software is capable of producing two sets of random numbers with the desired joint correlation statistics, with a specified center frequency and bandwidth, given the sample rate of the AWG. The IF signals produced by the AWG are then mixed up to the desired RF passband of 10.6-10.65 GHz by a pair of up-conversion modulators. The net result is a pair of signals whose individual brightness temperatures can be adjusted anywhere between 150 K and 350 K and whose real and imaginary components of correlation can independently be adjusted anywhere between 0 K and 200 K.

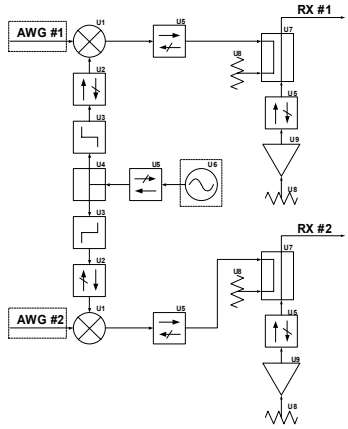

Figure 1. Two active cold loads provide uncorrelated noise backgrounds for two separate channels. Components common to both channels include the LO and the AWG that are the largest sources of introduced error.

The CNCS was designed and originally used as a laboratory calibration tool during the integration and testing of correlating receivers for the Lightweight Rainfall Radiometer (LRR) Fourier synthesis imager [2]. The results and analysis presented here represent a new use for the CNCS – to calibrate a fully polarimetric radiometer. The Airborne Earth Science Microwave Imaging Radiometer (AESMIR), a NASA Goddard instrument that is fully polarimetric at 10.7 GHz, was calibrated using CNCS. The AESMIR instrument includes channels at 10.65, 18.7, 23.8, 36.5 and 89.0-GHz that are all housed in a common drum designed for airborne flight mounted on the exterior of a P-3 aircraft. Fully polarimetric channels are formed in the 10.65 GHz (and other) receiver by a hybrid combining network. V- and H-pol signals from the antenna are added together with a relative phase shift of 0^o, 90^o, 180^o, and 270^o to generate $+45^o$ slant linear (T_P), left hand circular (T_L), -45^o slant linear (T_M), and right hand circular (T_R) polarizations, respectively. The individual V- and H-pol signals are also individually detected, to measure the first and second modified Stokes brightness temperatures (T_Bs). Third and fourth Stokes T_Bs are computed during post processing by $T_3 = T_P - T_M$ and $T_4 = T_L - T_R$.

II. MEASUREMENT METHODOLOGY

A. CNCS Active Cold Load Calibration

The brightness temperatures of the active cold loads were calibrated prior to the AESMIR experiment using LRR receivers. Radiometric measurements were made of: 1) a warm reference blackbody load with T_B = 293.1 K; 2) a cold reference blackbody load in an LN_2 dewar with T_B = 82.3 K; 3) the active cold load; and 4) the active cold load with its bias voltage removed, in which case it acts like a blackbody load at a regulated physical temperature of 308 K. Because the effective brightness of the active cold load includes loss and thermal emission by interconnecting cables, all measurements were made with the same low-loss coaxial cables as were used to connect the CNCS to AESMIR.

B. AESMIR Calibration

The CNCS polarimetric measurements were made on a laboratory bench top without AESMIR's drum housing or external calibration load assembly. Some other form of system level calibration was needed in order to track and correct for slow drifts in receiver gain and offset. This was done with periodic hot and cold black body reference measurements that were provided by the CNCS by turning off the AWG signal. In addition, a third measurement was also made, with the active cold load off (*i.e.* hot) and the local oscillator (LO) that pumps the upconversion modulator also turned off. This third measurements allows for correction of a small correlated signal of several Kelvin that is introduced by LO leakage into AESMIR. These three calibration measurements were repeated before and after each of the polarimetric calibration tests.

C. Input Signal Nomenclature

A pair of CNCS signals is injected into the AESMIR receiver in place of the two (V- and H-pol) outputs from its antenna. The raw data recorded by AESMIR include one second averaged square law detector voltages for each of the T_V, T_H, T_P, T_M, T_L and T_R channels. A very large number of possible polarization states and T_B magnitudes can be generated by CNCS. In order to simplify the description of the states, we use several notation conventions. The correlation coefficient between the pair of CNCS signals has magnitude $|R_{vh}|$ and phase θR_{vh}. The equivalent brightness temperature of the component of the CNCS signal that is generated by the AWG is T_{AWG}. These definitions result in the following relationships:

i. $T_V = T_H = 150\ K + T_{AWG}$, where the 150 K offset results from the background brightness temperature of the active cold loads and where the magnitudes of the two AWG signals are assumed to be the same.

ii. $\sqrt{T_3^2 + T_4^2} = |R_{vh}|T_{AWG}$, where T_3 and T_4 are the 3rd and 4th Stokes brightness temperatures measured by AESMIR (assuming an ideal hardware response).

iii. The phase angle, θR_{vh}, will orient a vector with magnitude $\sqrt{T_3^2 + T_4^2}$ in complex (T_3, T_4) space according to $T_3 = |R_{vh}|\cos(\theta R_{vh})$ and $T_4 = |R_{vh}|\sin(\theta R_{vh})$.

III. CNCS NON-IDEAL CHARACTERISTICS

A. LO Leakage Characterization

The LO leakage represents the largest component of correlated signal leakage as the LO signal is common to both signal paths. Table I shows that the injected LO signal does vary throughout the measurement period. To obtain more accurate measurements in future, it would be necessary to use a lower jitter oscillator. In the T_3 and T_4 plane, the correlation phase also varies slightly. The uncertainty introduced by the LO leakage is on the order of 0.20 K.

TABLE I. LO SUMMARY

	T_v LO	T_h LO	T_3 LO	T_4 LO	T_{CORR} Mag.
Magnitude, K	1.91	0.46	4.16	3.93	5.73
Std Dev, K	0.20	0.17	0.26	0.22	0.26

B. AWG Leakage Characterization

After the removal of the LO leakage, the correlated component of the AWG signal can be found by plotting the T_3 and T_4 components for various partial correlation magnitudes and angles, and determining their center. Fig. 2 is generated for constant front panel voltage amplitude, varying partial correlation magnitudes and angular steps of 90° (45°, 135°, 225°, 315°). By grouping the points that are 180° out of phase, we are able to determine the intersection point, the point of supposed zero correlated signal, to a high degree. For this set of data the intersection occurs at (-0.57, 2.74). Given this, it is possible to 'center' the intersection to remove for the residual correlation from the AWG and the radiometer system. It is important to note that while the signals are 90° apart, there remains an offset angle for the correlation phase. This $\Delta\theta R_{vh}$ is found to be approximately -31.8°.

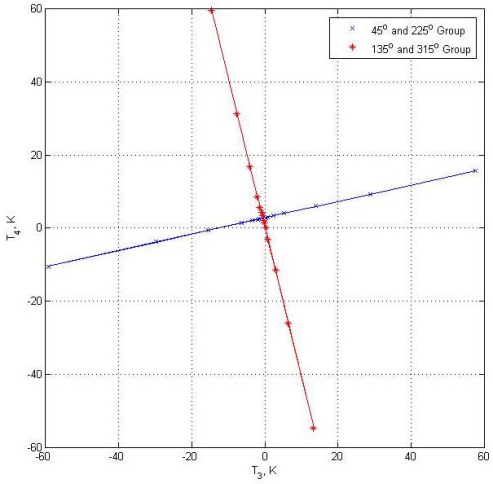

Figure 2. Grouped results with correlation phase differing by 180° plotted on the T_3 and T_4 plane. The intersection point determines the residual correlation, while the skew from the axis, the phase deviation.

While processing the data for the 0°, 90°, 180° and 270° dataset, taken over the span of two days, we observe an issue. The measurement made for the lower left quadrant in Fig. 3 was performed during the second day of data collection. While general calibration is performed for the radiometer system

using the CNCS hardware and remains stable, it appears that the output of the AWG has drifted significantly lower over time. For future iterations of the CNCS it would be valuable to build a feedback system that would monitor the output of each channel from the AWG and keep this output value constant and stable for both channels over longer periods of time. However the data products are still useful since they are calibrated independently of the AWG. The intersection point is not exactly consistent over both days since the output characteristics of the AWG have changed. For both these plots the R^2 value, where R^2 is the fractional explained variance of the linear regression fit (correlation coefficient of the fit), of the linear fit lines are over 0.999.

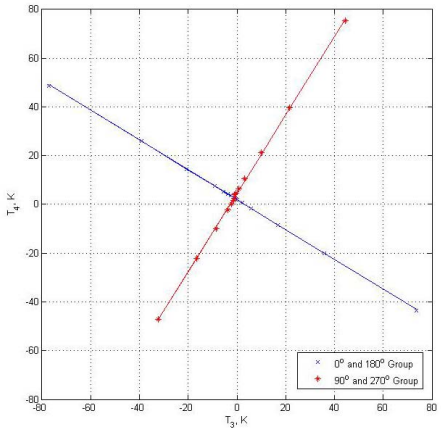

Figure 3. Measurements made over 2 different days show that the AWG output has drifted over time. The measured magnitude in the lower left quadrant, performed during the second day, is significantly lower.

C. Partial Correlation Linearity Verification

Fig. 4 presents the relationship between the partial correlation magnitude and the generated $\sqrt{T_3^2 + T_4^2}$. It is clearly seen that the magnitude changes linearly as expected. Deviation from the linearity occurs at the lower levels due to the effects of the radiometer system and uncorrected residual AWG signal. Note that the measured magnitude is much less than the input correlation magnitude due to the effects of the uncorrelated background signal produced by the two separate active cold loads.

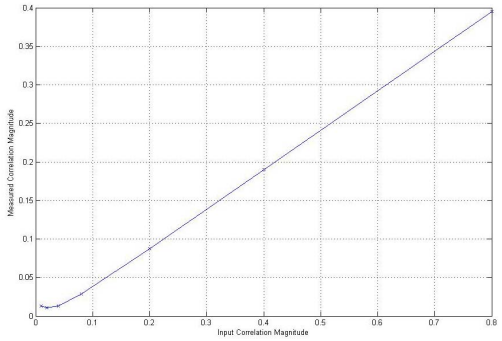

Figure 4. Measured correlation magnitude vs input correlation magnitude.

IV. AESMIR Preliminary Data Products

Using the CNCS, we can now inject a variety of signals into the radiometer, and as shown by the following results, demonstrate its usefulness and flexibility including its ability to determine the quality of data retrieved. In addition to acting as a simple total power calibration tool, we are also able to test the linearity of the channels, as well as exercise the inputs with varying levels of R_{vh}, partial correlation magnitude, ρ_{vh}, and angle, θ_{vh}. Bear in mind that additional work needs to be done to fully remove the residual effects of the CNCS hardware, any other systematic error in the current CNCS system that has not been fully accounted for in this process.

A. Polarimetric Channel Output Measurements

For correlation measurements, we are able to vary both the correlation amplitude and the phase easily using the CNCS system. Variation of θR_{vh} in 45^0 steps shows the versatility of the CNCS system. Fig. 5 shows a plot of the measured T_B from the T_P, T_M, T_L and T_R channels against varying θR_{vh}. It can clearly be seen that the channels differ in phase by approximately 90^0 and are centered on a mean brightness temperature value. The sinusoidal shape is also evident.

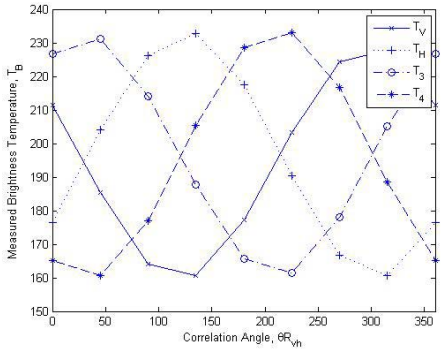

Figure 5. Correlated channel outputs against correlation angle. The four channels can be seen to be separated by 90^0 and centered over a mean value.

The modulus of the correlated brightness $\sqrt{T_3^2 + T_4^2}$ also remains stable throughout these measurements as only θR_{vh} is varied. Fig. 6 displays all four Stokes parameters with T_V and T_H stable while T_3 and T_4 are varying sinusoidally.

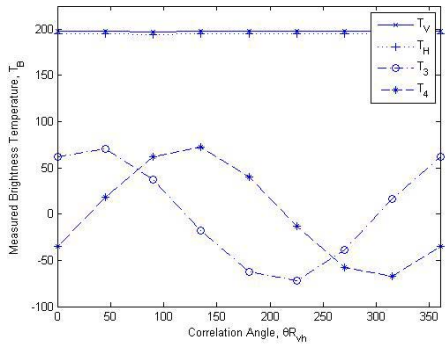

Figure 6. Stokes brightness temperatures against correlation angle. V- and H-Pol temperatures do not vary since only the correlation angle is varied.

B. *Calibrated Polarimetric Outputs*

Variations from the ideal for the correlated products are offsets in both phase and magnitude. Using the methods outlined prior to remove the LO leakage and the residual correlated signals, we are then able to re-center the measurements in the complex plane. Fig. 7 shows a calibrated circle plotted on the complex (T_3, T_4) plane. The effects of the LO leakage, the residual correlated signal, and the angular offset ($\Delta\theta R_{vh}$), have been removed. Points are distributed uniformly around the circle at 45^0 angles at the two levels of AWG output signal. Since the correlation magnitude is constant, the circle maintains a constant radius during this measurement set. The upper voltage level is set to be approximately double the power output of the lower voltage level. It can be seen that the radius of the outer circle is double that of the inner one.

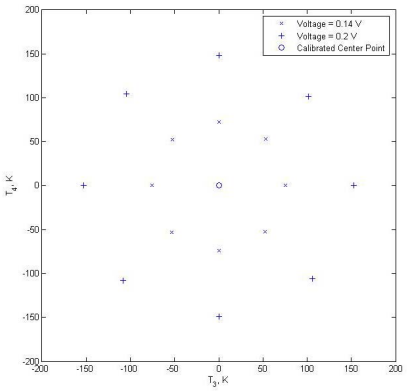

Figure 7. Calibrated T_3 and T_4 values at 45^0 steps and two power levels. The upper power level is double that of the lower power level which can be seen as the outer circle has double the radius of the inner circle.

C. *Radiometer Gain Matrix*

From these measurements, we are then able to determine the full gain matrix of the radiometer.

$$\begin{pmatrix} V_v \\ V_h \\ V_p \\ V_m \\ V_l \\ V_r \end{pmatrix} = \begin{pmatrix} G_{vv} & G_{vh} & G_{v3} & G_{v4} \\ G_{hv} & G_{hh} & G_{h3} & G_{h4} \\ G_{pv} & G_{ph} & G_{p3} & G_{p4} \\ G_{hv} & G_{hh} & G_{h3} & G_{h4} \\ G_{lv} & G_{lh} & G_{l3} & G_{l4} \\ G_{rv} & G_{rh} & G_{r3} & G_{r4} \end{pmatrix} \begin{pmatrix} T_v \\ T_h \\ T_3 \\ T_4 \end{pmatrix} + \begin{pmatrix} O_v \\ O_h \\ O_p \\ O_m \\ O_l \\ O_r \end{pmatrix} \quad (1)$$

The offset for each row in Eqns. (1) represents the receiver temperatures for each radiometer channel that have already been determined earlier. In order to solve for this equation fully, a set of five measurements must be made to determine the five unknowns for each row. Components include hot and cold measurements to determine channel offsets, varying hot and cold measurements to determine cross polarization gains and varying correlated noise measurements to determine 3rd and 4th Stokes gain coefficients. This will ensure that they system of equations are full rank. Preliminary results for the AESMIR gain matrix are presented in Table II.

TABLE II. PRELIMINARY AESMIR GAIN MATRIX VALUES

Gain Matrix, Units of mV/K				
	v	h	3	4
v	12.68	0.00	0.00	0.00
h	0.00	9.18	0.00	0.00
p	5.28	5.64	5.41	-0.02
m	5.63	6.01	-5.99	-0.02
l	6.16	5.92	-0.20	6.43
r	5.91	5.68	-0.19	-5.98

V. CONCLUSIONS

The X-Band CNCS was demonstrated using AESMIR, a microwave radiometer at GSFC. During the two days of tests, the system made over 18 different measurements utilizing data files that had varying levels of partial correlation and correlation phase. Calibration of the radiometer was performed using the CNCS since AESMIR relied on calibration targets that were only available when the system was fully integrated.

LO leakage was characterized using the calibration data and was found to be relatively stable in terms of magnitude and phase to 0.2 K. Grouping of measurements that were 90^0 out of phase in the T_3 and T_4 plane allowed determination of AWG unwanted magnitude and phase via the intersection of the lines of best fit. The output of the AWG drifted significantly between the first and second days. Interpretation of the data is still possible as the measurements are calibrated against values that do not depend on the AWG output levels.

Datasets looking at varying levels of correlation magnitude showed both an upper and lower limit of correlation. The upper limit is due to the presence of the uncorrelated background signal originating from the two separate active cold loads. The lower limit is due residual correlation from the radiometer system and the AWG.

A method is developed to determine the gain matrix of the system. By applying the correct set of measurement results, it is possible to solve for the gain matrix. Additional results with valuable information, such as the cable swap measurements and measurements against other radiometers have not been integrated yet.

Results presented here show that the CNCS is able to exercise fully all the channels of the polarimetric system. The flexibility in varying input power levels as well as correlation magnitude and phase with high resolution allow for detailed testing of radiometer hardware.

VI. REFERENCES

[1] Ruf, C.S. and J. Li, "A Correlated Noise Calibration Standard for Interferometric, Polarimetric and Autocorrelation Microwave Radiometers," IEEE Trans. Geosci. Remote Sens., 41(10), 2187-2196, 2003.

[2] Li, J. and C.S. Ruf, "Correlated Noise Calibration System for a Multichannel Interferometric Radiometer," Proc. of the First International Microwave Radiometer Calibration Workshop, Adelphi, MD, 30-31 Oct 2000.